J-PARCイメージング装置 RADENの現状

日本原子力研究開発機構　J-PARCセンター
篠原　武尚
takenao.shinohara@j-parc.jp

螺鈿装置メンバー
甲斐哲也、及川健一、中谷健、廣井孝介、蘇玉華、
關義親、土川雄介（J-PARC）
林田洋寿、J.D. Parker、松本吉弘、桐山幸治 (CROSS)
鬼柳善明（名古屋大）

Neutron imaging

Fundamental technique to observe inner structure/behavior of object by means of neutron transmission measurements.

Light/heavy elements
Large objects
Magnetic sensitivity

4800RPM, 2000FPS
TNRF@JRR-3

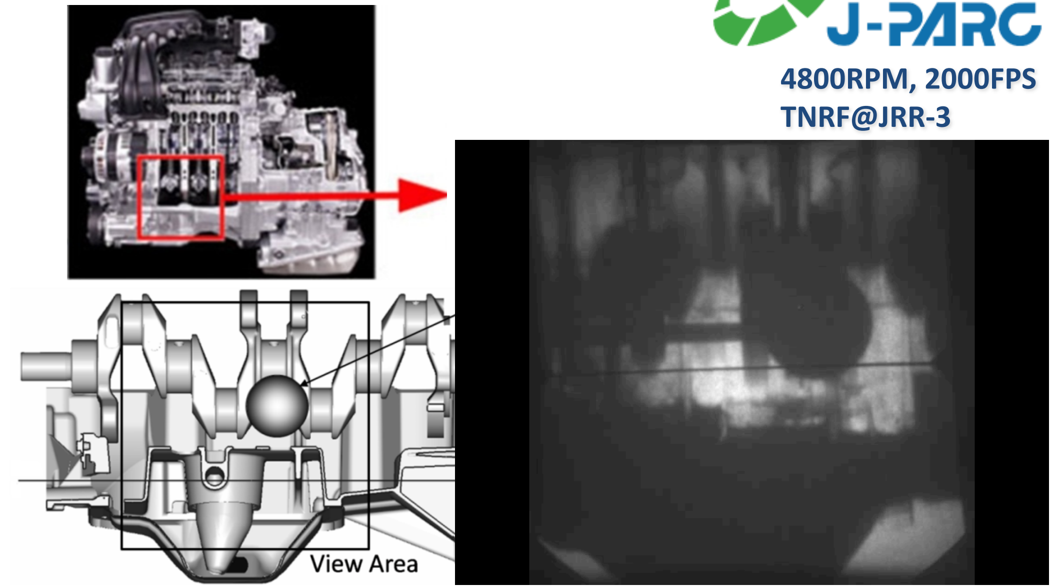

Motion of oil in a car engine

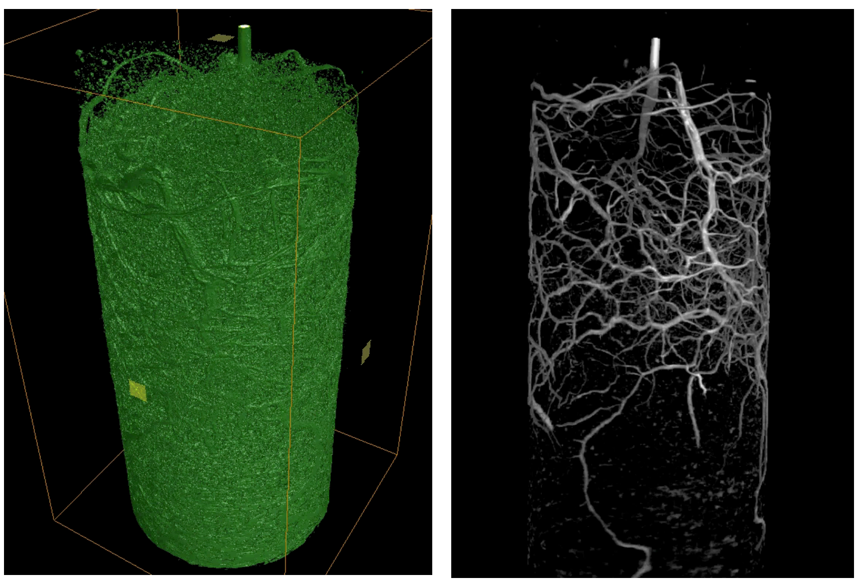

Roots of soy bean

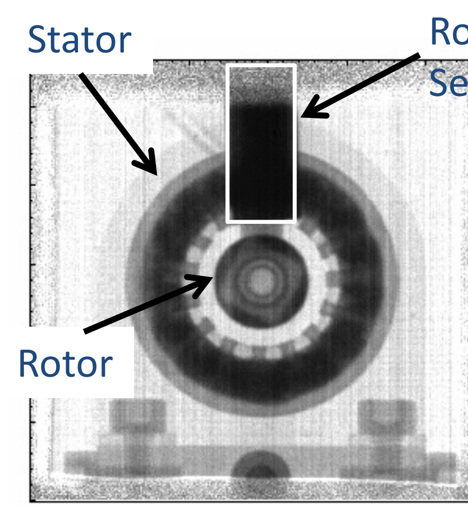

Neutron Radiograph

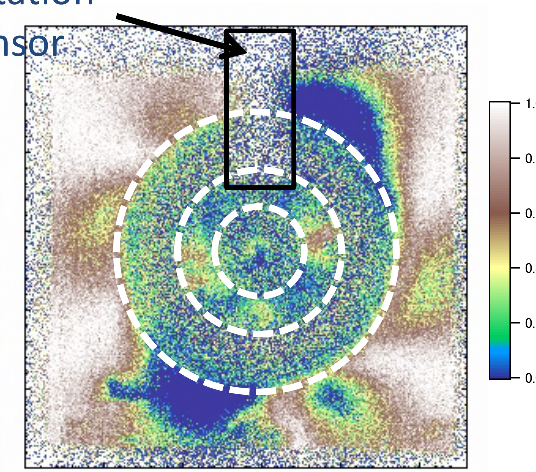

Polarization image

Model electric motor f=21.5Hz

Steady Source? Pulsed Source?

Steady source

Research Reactor

Constant neutron intensity

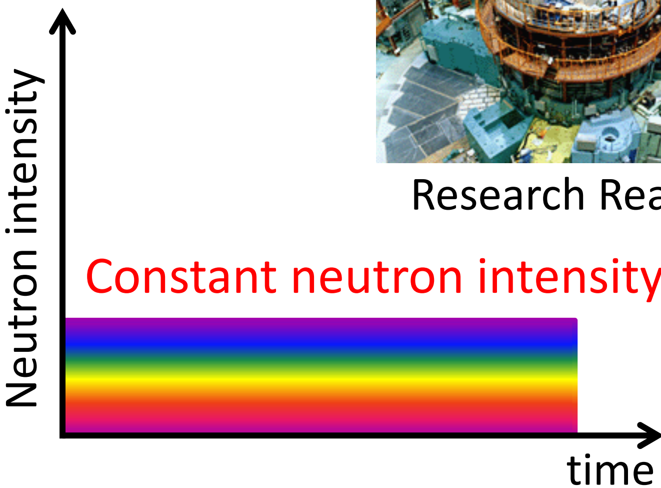

- High neutron flux
- White beam
- No time structure

Pulsed source

Accelerator based source

J-PARC
SNS
ISIS
ESS

Periodical neutron generation

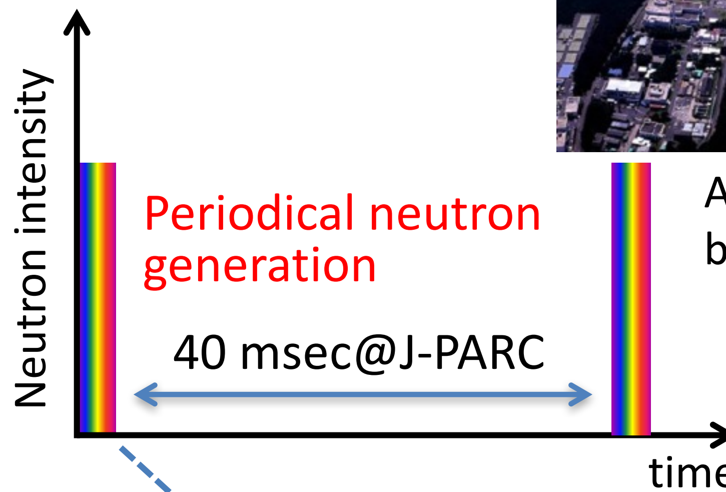

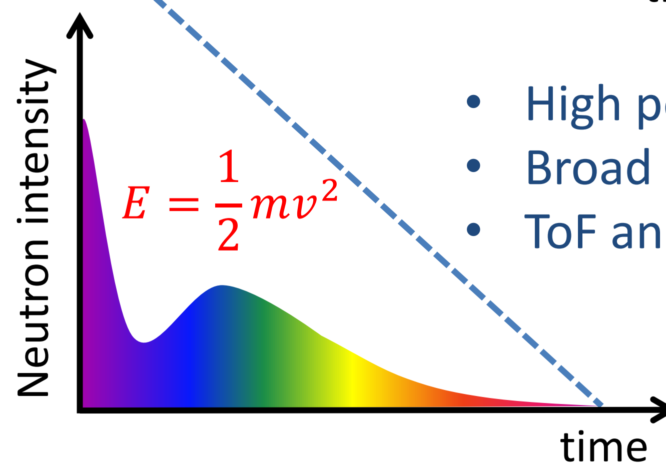

- High peak intensity
- Broad energy range
- ToF analysis

Time of Flight of a neutron
→ Neutron Energy

Pulsed neutron is suitable to analyze wavelength/energy dependent phenomena.

Neutron imaging using pulsed neutrons

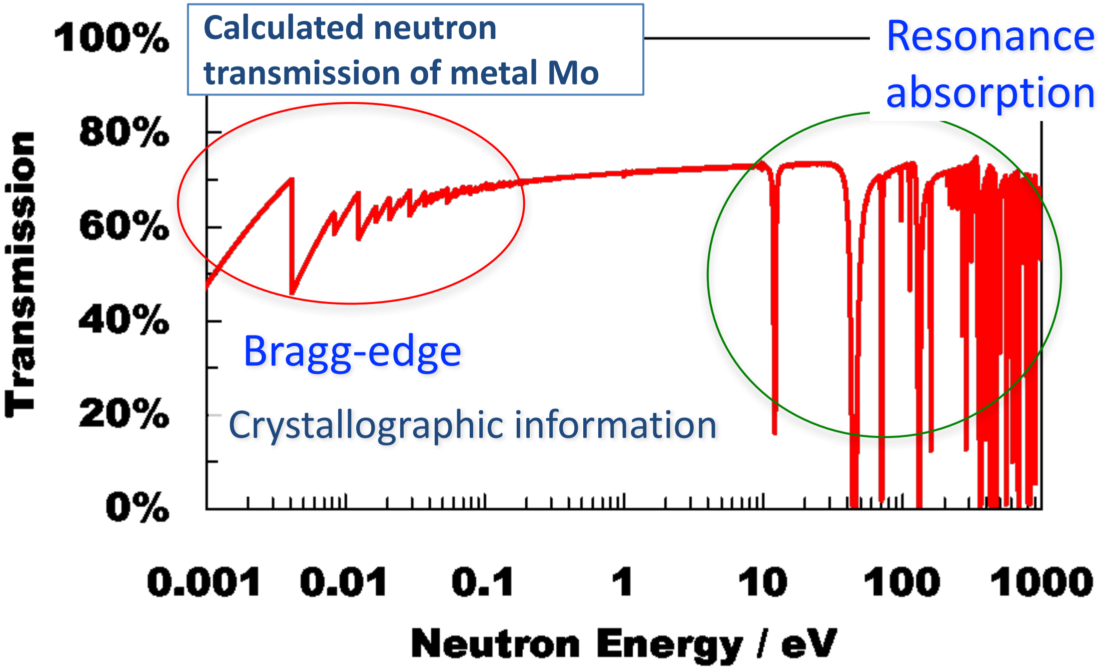

Elemental & thermal information

Natural Gold Single Crystal Samples

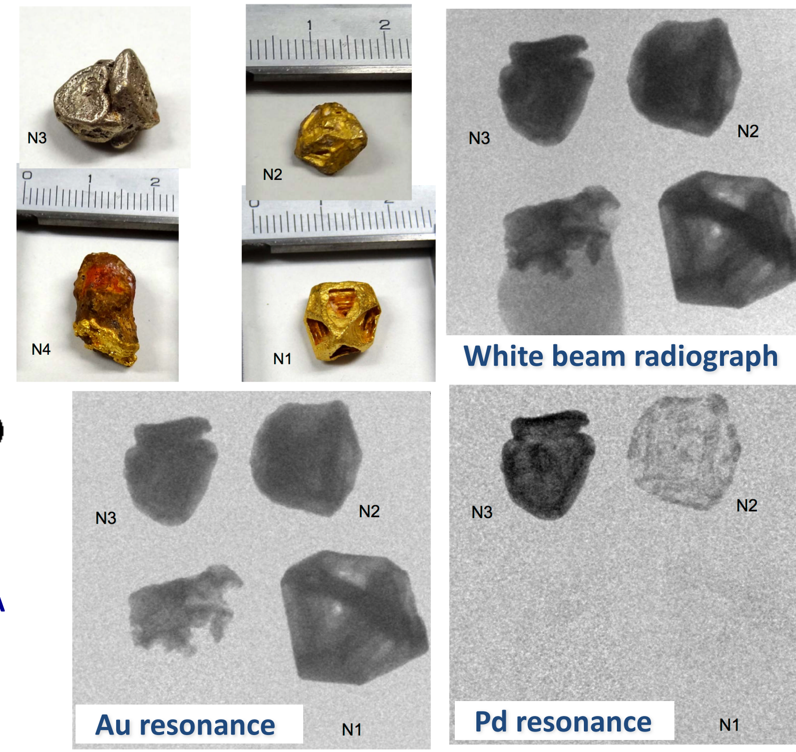

Scientific Report 7 (2016) 40759

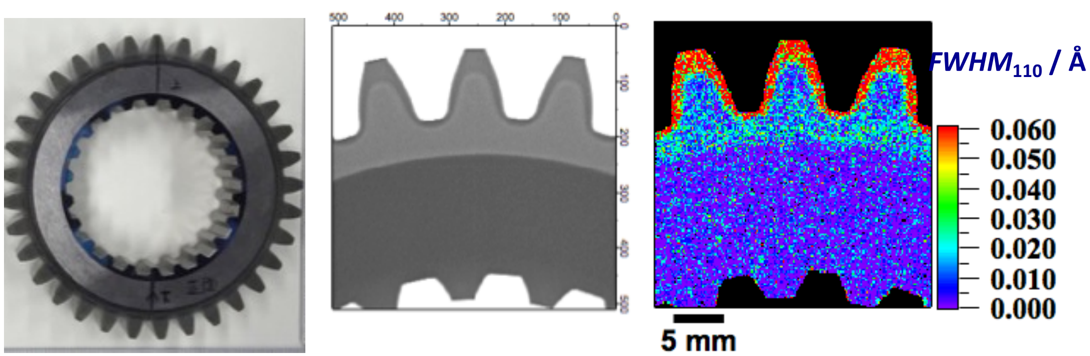

Steel Gear White beam radiograph Lattice parameter

Pulsed neutron is suitable for energy-resolved imaging.

- ✓ Effective measurements by TOF
- ✓ Fine wavelength resolution
- ✓ Wide wavelength/energy range

J-PARC -Japan Proto omplex-

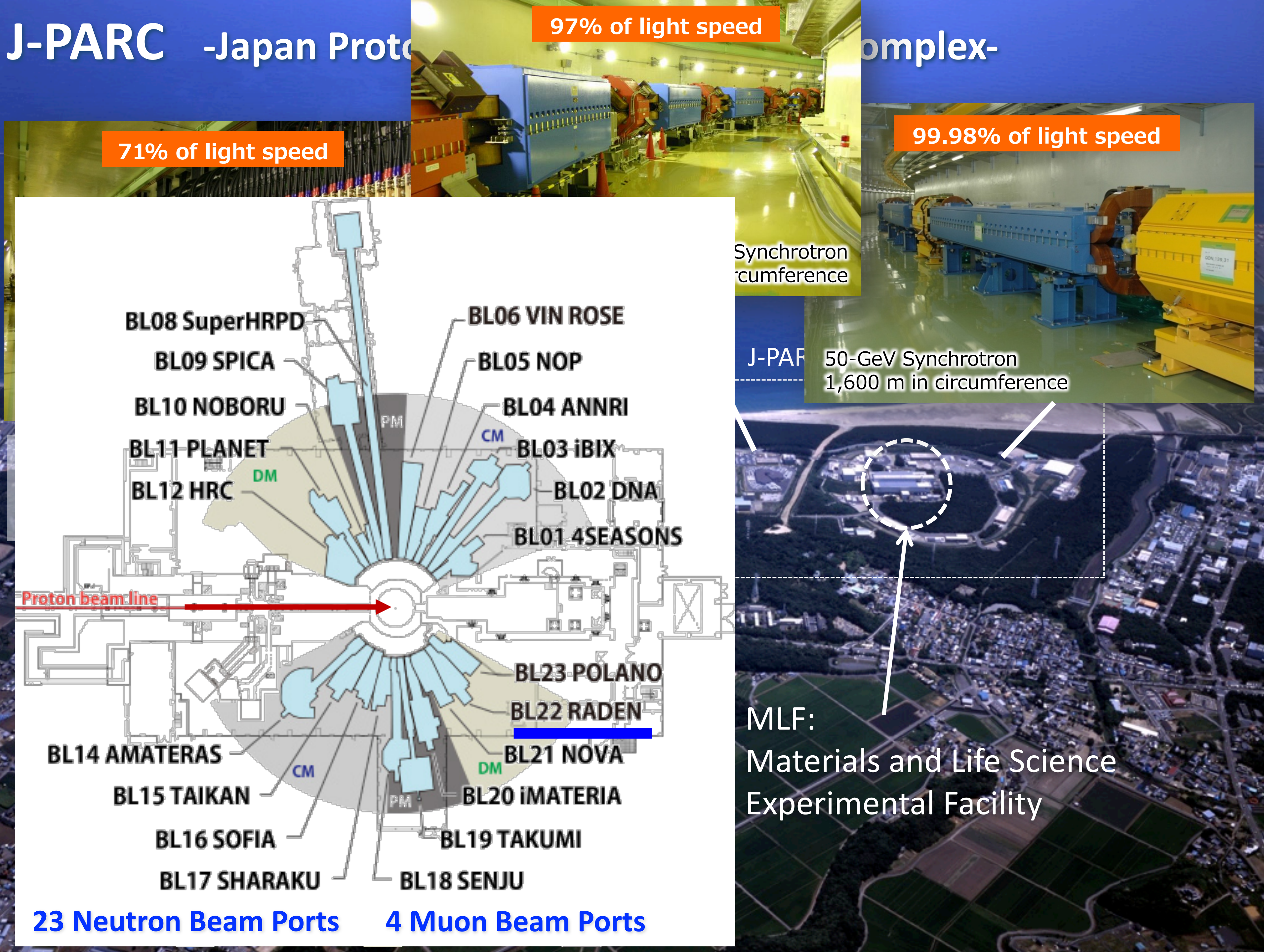

Energy-Resolved Neutron Imaging System “RADEN（螺鈿）” at J-PARC MLF

世界最初のパルス中性子イメージング専用ビームライン

エネルギー分析型中性子イメージング装置

・パルス中性子の特徴を活かした新しいイメージング

→核種情報・結晶組織情報・温度情報・磁場情報

高性能中性子ラジオグラフィ装置

・FOVと空間分解能に応じて検出器を選択可能

・高速CT再構成用計算環境を整備

・大型試料、特殊環境、その場観察の実験環境

新しい中性子イメージング技術開発環境

Construction started in 2012 and completed in Nov. 2014.

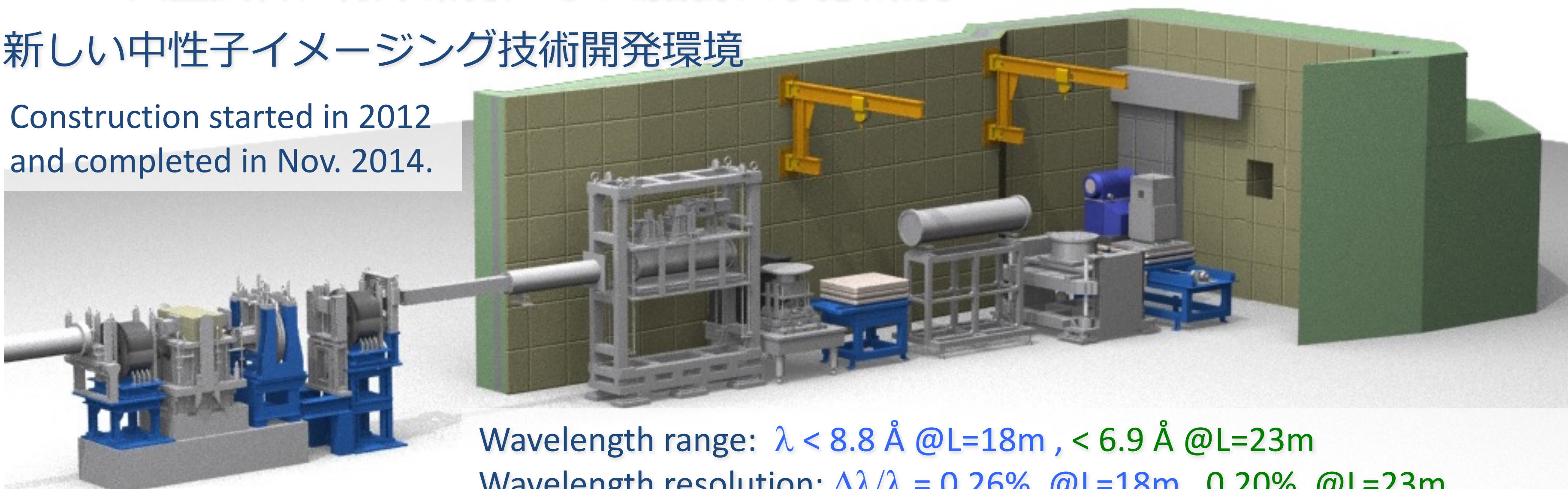

Wavelength range: λ < 8.8 Å @L=18m , < 6.9 Å @L=23m

Wavelength resolution: $\Delta\lambda/\lambda$ = 0.26% @L=18m , 0.20% @L=23m

Time averaged neutron flux (< 0.45 eV): 2.6 x 10^7 n/sec/cm^2@L/D=180

User Program Status - from 2015A to 2019B-

Approved beam time (days)

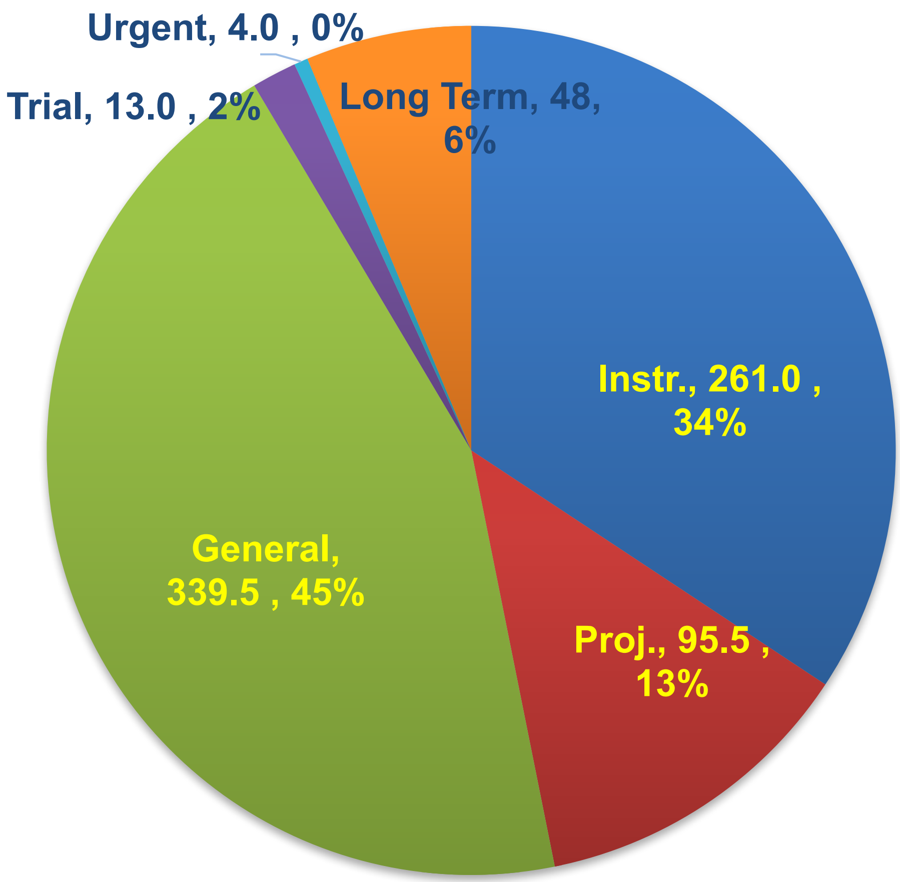

Proposal number percentage of each technique

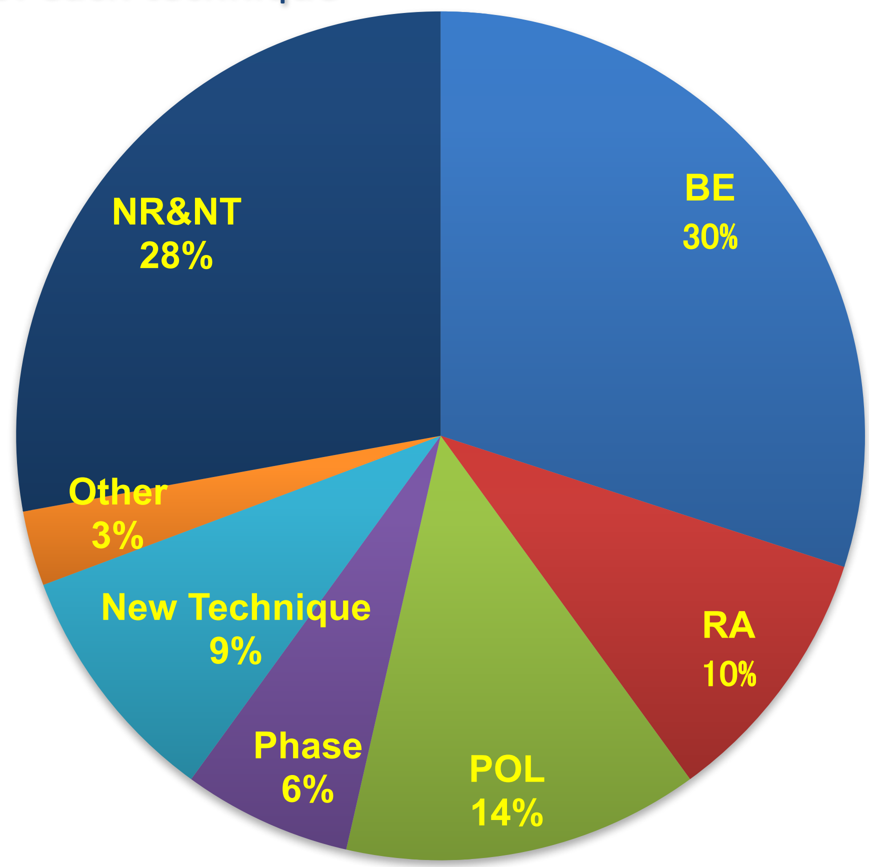

Proposal number
Submitted : 178
Approved : 145
(Adoption rate = 0.81)

NR & NT : Conventional
BE : Bragg Edge
RA : Resonance Absorption
POL : Polarized Neutron
Phase : Phase Imaging
Technique : Development

J-PARC/MLF

User Program Status -Annual trends-

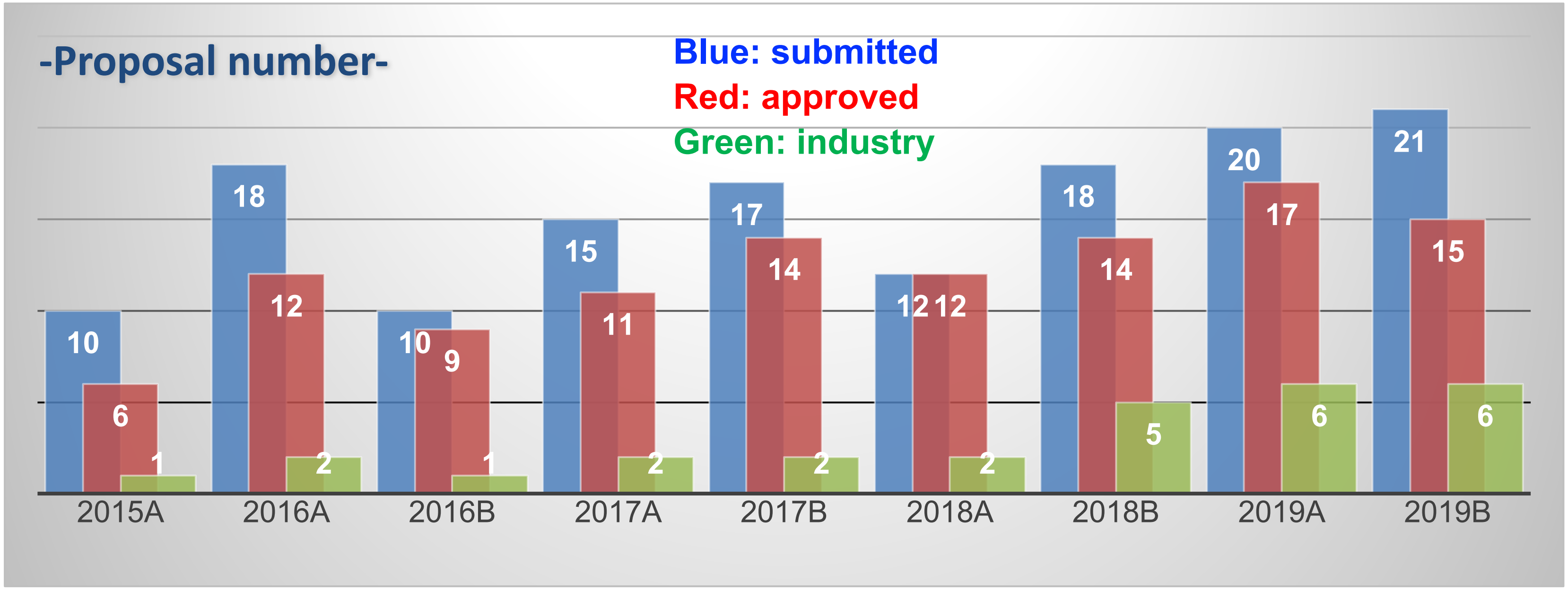

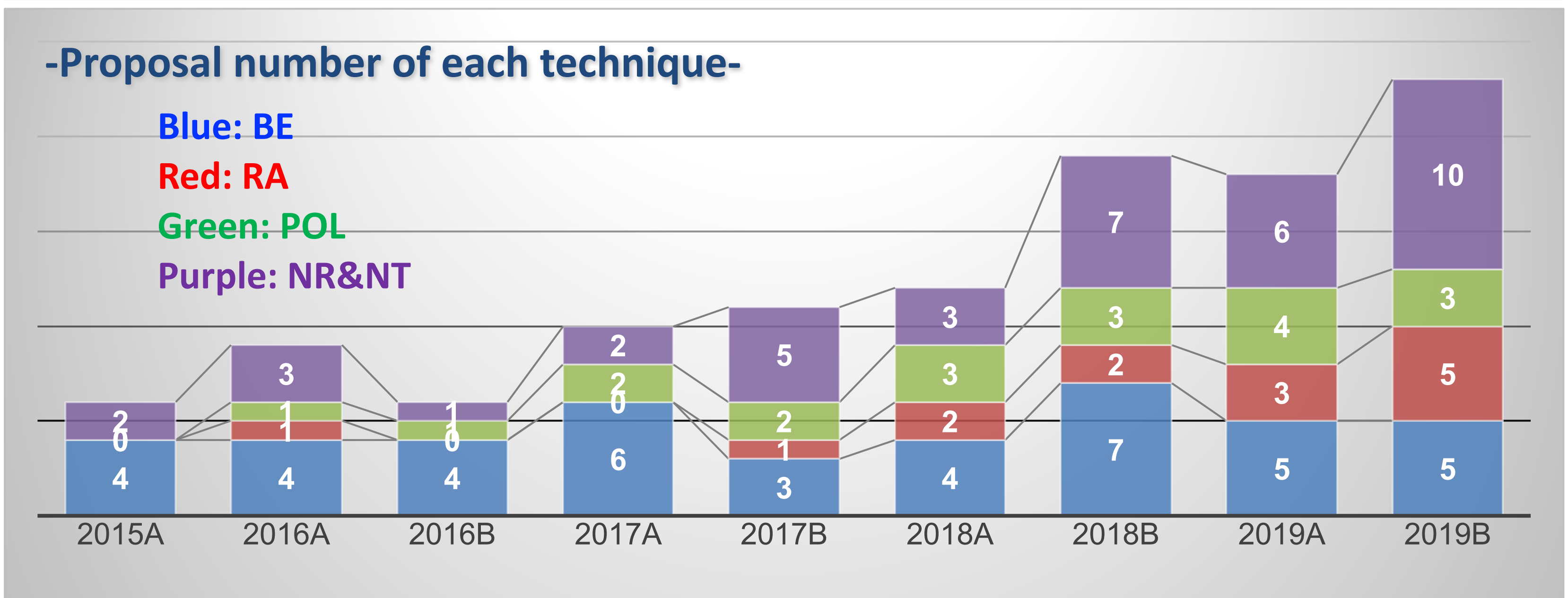

J-PARC/MLF

Strain Tomography by Bragg-edge imaging

Strain caused by one dimensional deformation

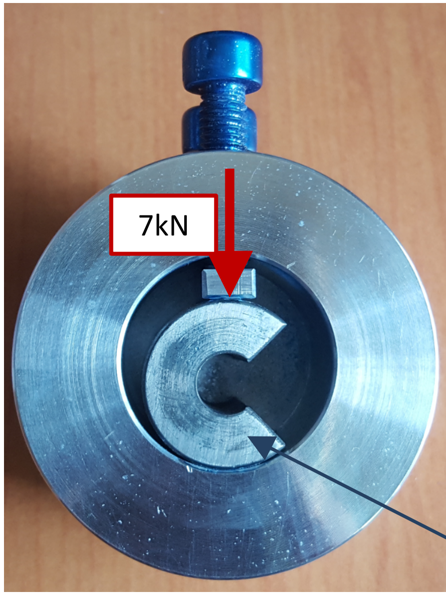

Bragg edge shift + displacement information

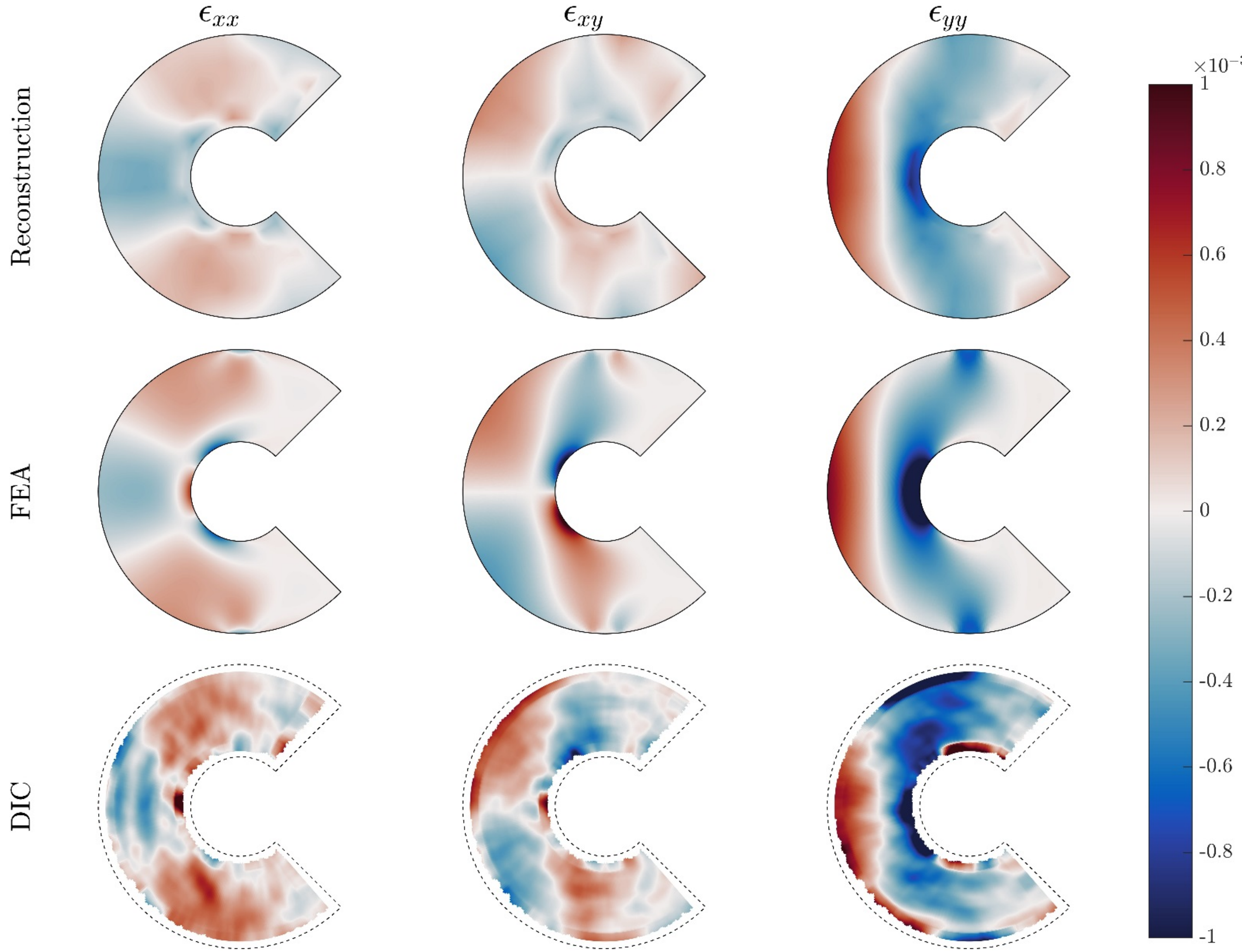

Sample: C-shaped Steel (EN26) + Al jig
Detector: MCP detector (A. Tremsin)
Projection number: 86

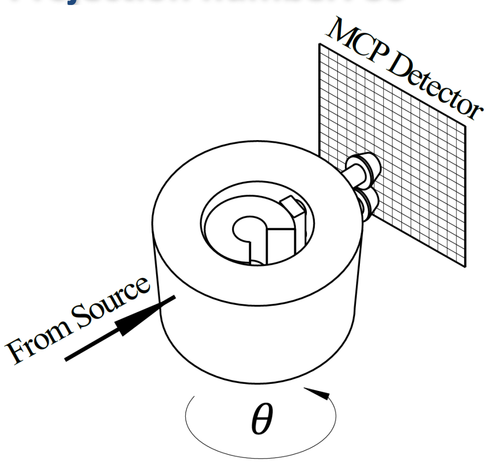

Chris Wensrich et al. @ Univ. Newcastle

J. N. Hendriks, et al. Phys. Rev. Mater., 1, 053802 (2017)

Courtesy of Chris Wensrich (Univ. Newcastle)

Experiment #2: 2D Residual Strain Fields

Strain tomography experiment at J-PARC (Jan 2018);

- Two 2D steel samples (1D projections)
- 50 strain projections from (110) Bragg-edge at golden angle increments (~4 days).

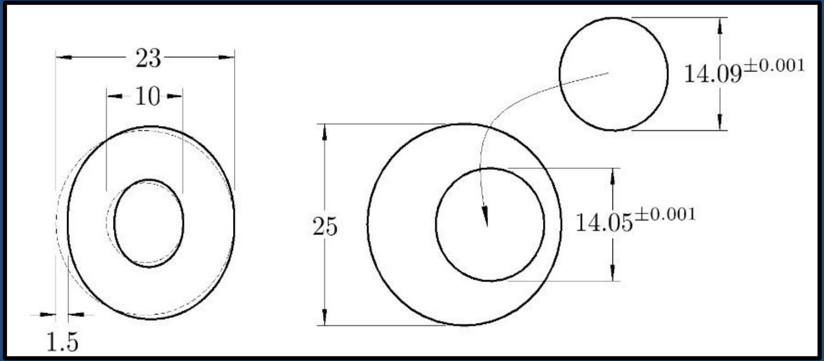

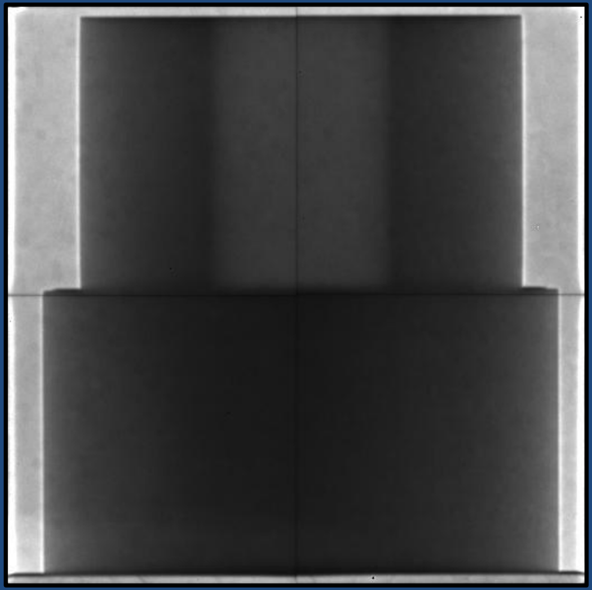

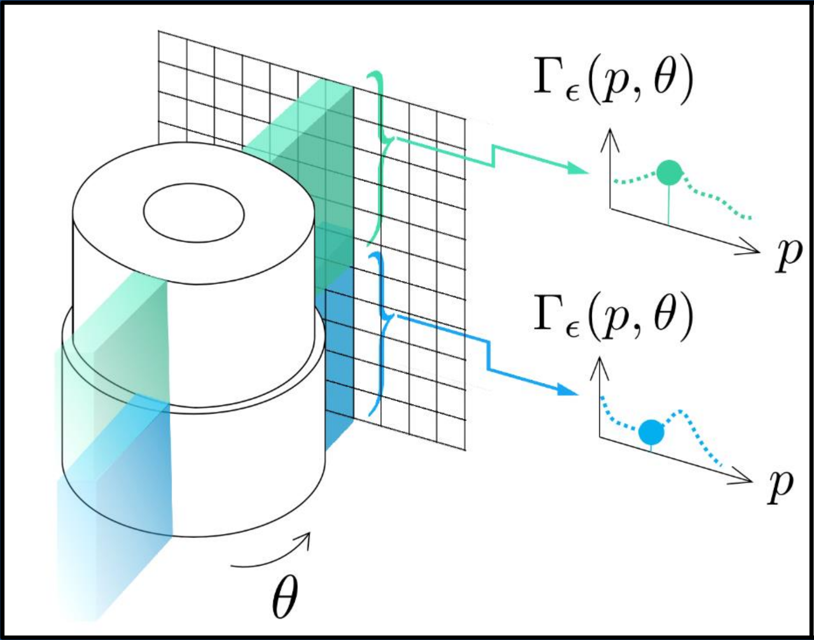

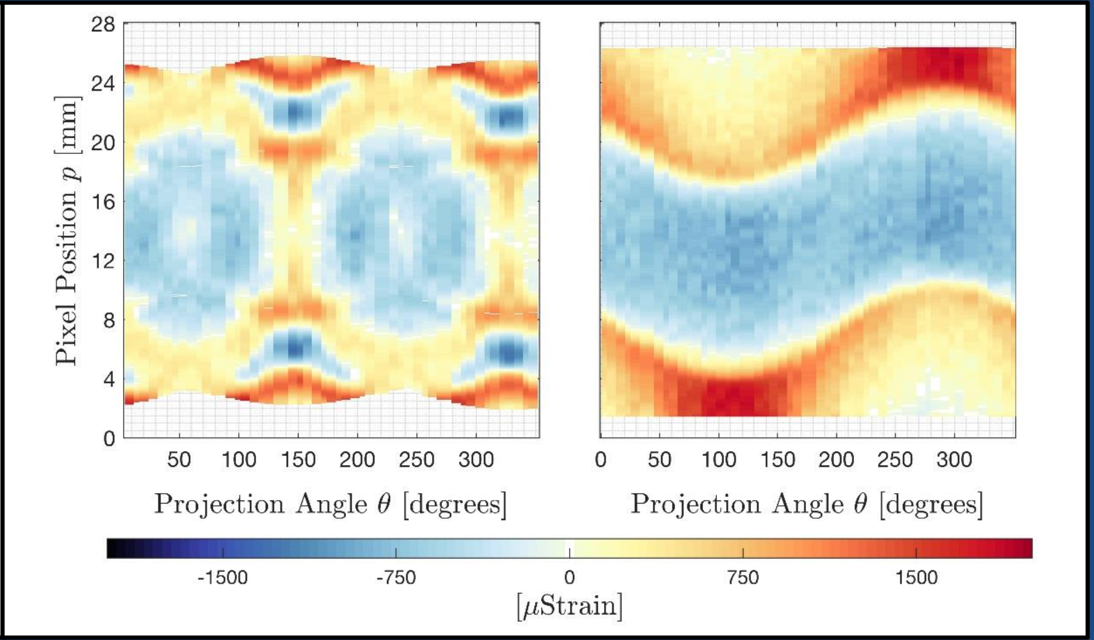

2D Proof-of-Concept: General 2D Reconstruction:

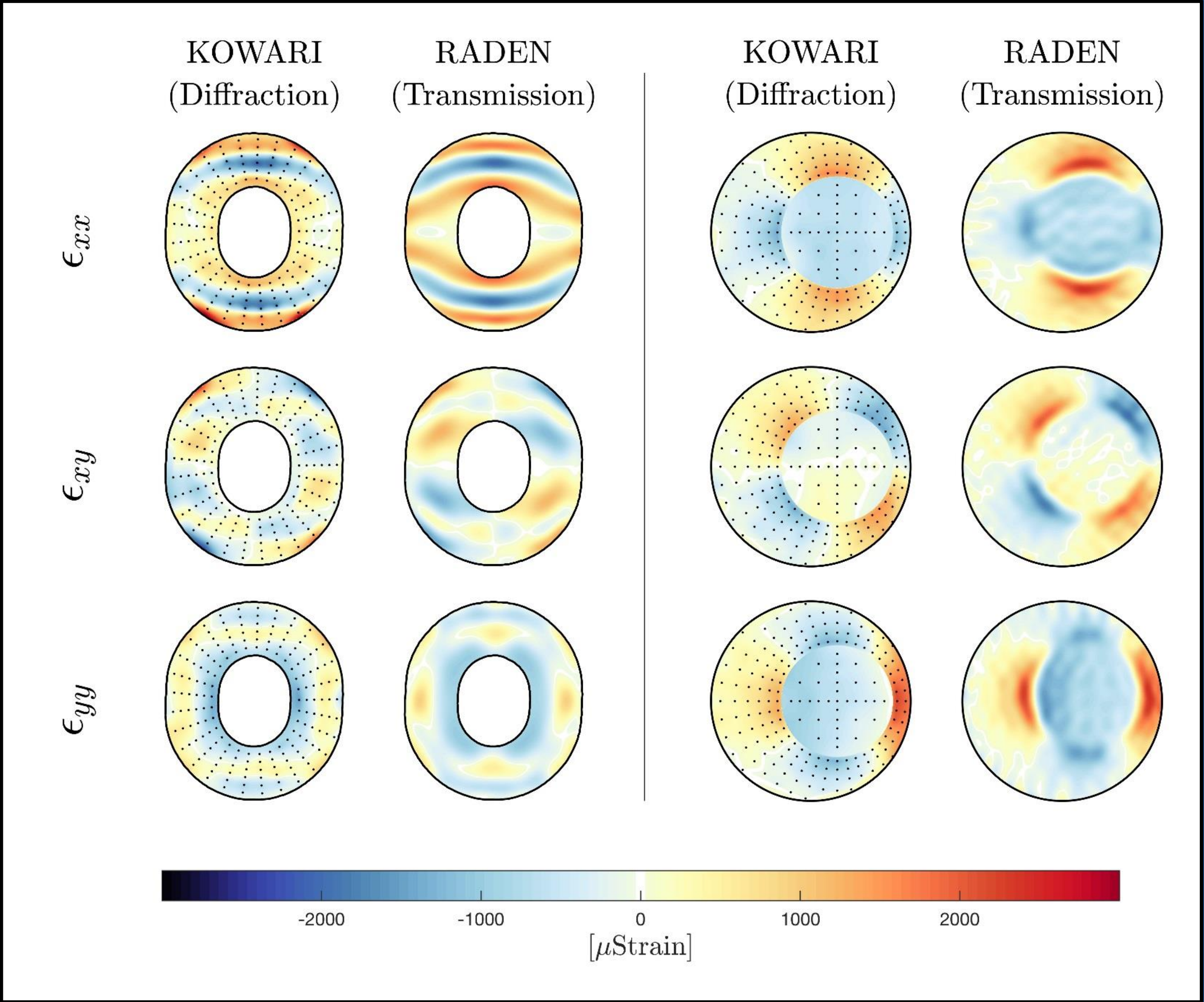

A Gregg, JN Hendriks, CM Wensrich, A Wills, AS Tremsin, V Luzin, T Shinohara, O Kirstein, MH Meylan, and EH Kisi, "Tomographic reconstruction of two-dimensional residual strain fields from Bragg-edge neutron imaging", Physical Review Applied (Submitted March 2018)

KOWARI Diffraction Measurements:

- 0.5x0.5x14mm
- 211 peak (α-Fe)
- $\lambda = 1.67$Å
- 147/195 points
- MATLAB 'Natural neighbour' Interpolation (ring separate from plug)

KOWARI ~6 days
RADEN ~4 days

Resonance absorption imaging

In situ observation of crystal growth

A. Tremsin, D. Perrodine
@UC Berkeley & LBNL

Understand and optimize growth process for single crystal materials.
-> Transfer that knowledge to industrial scale production.

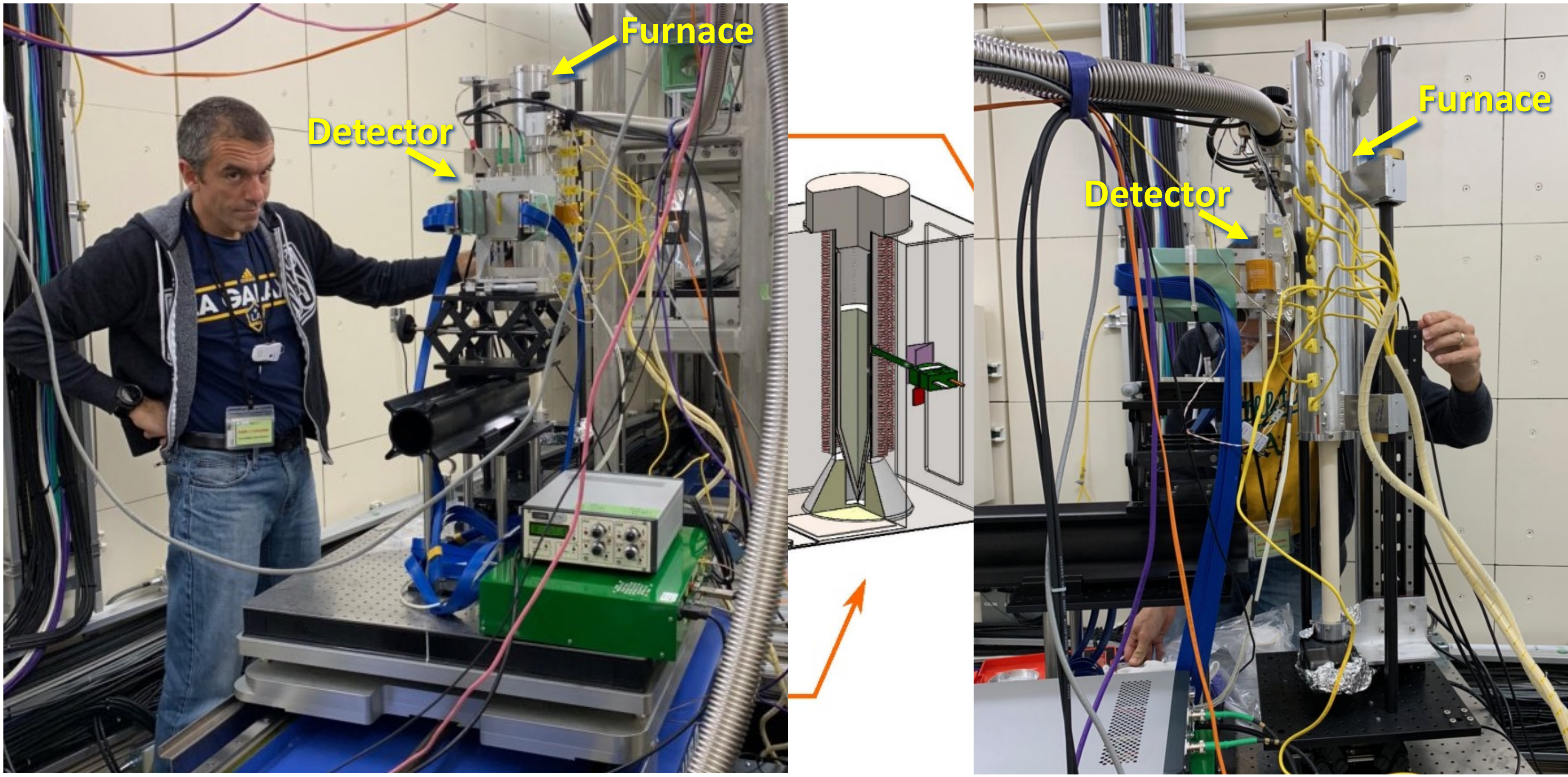

Phase separation during growth of $Cs_2LiLaBr_6$:Ce

Cryst. Growth Des. 17 (2017) 6372

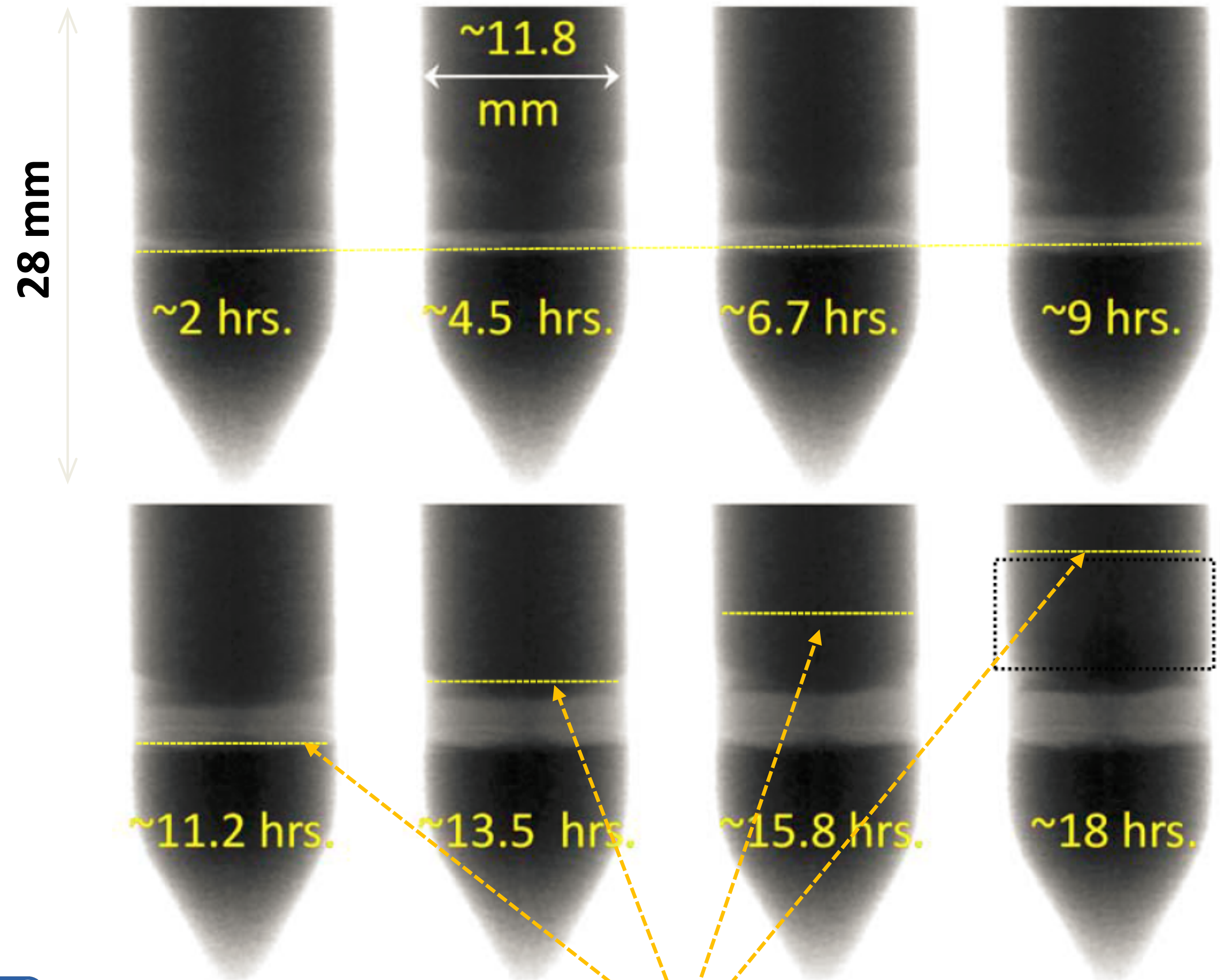

Steady T at 555 C first 11 hours

Growth over 7 hours at ~2 mm/hr. rate

Location of solid/liquid interface

Courtesy of Anton Tremsin
(UC Berkeley)

Phase separation during growth of $Cs_2LiLaBr_6$:Ce

Elemental composition map: Li concentration

Cryst. Growth Des. 17 (2017) 6372

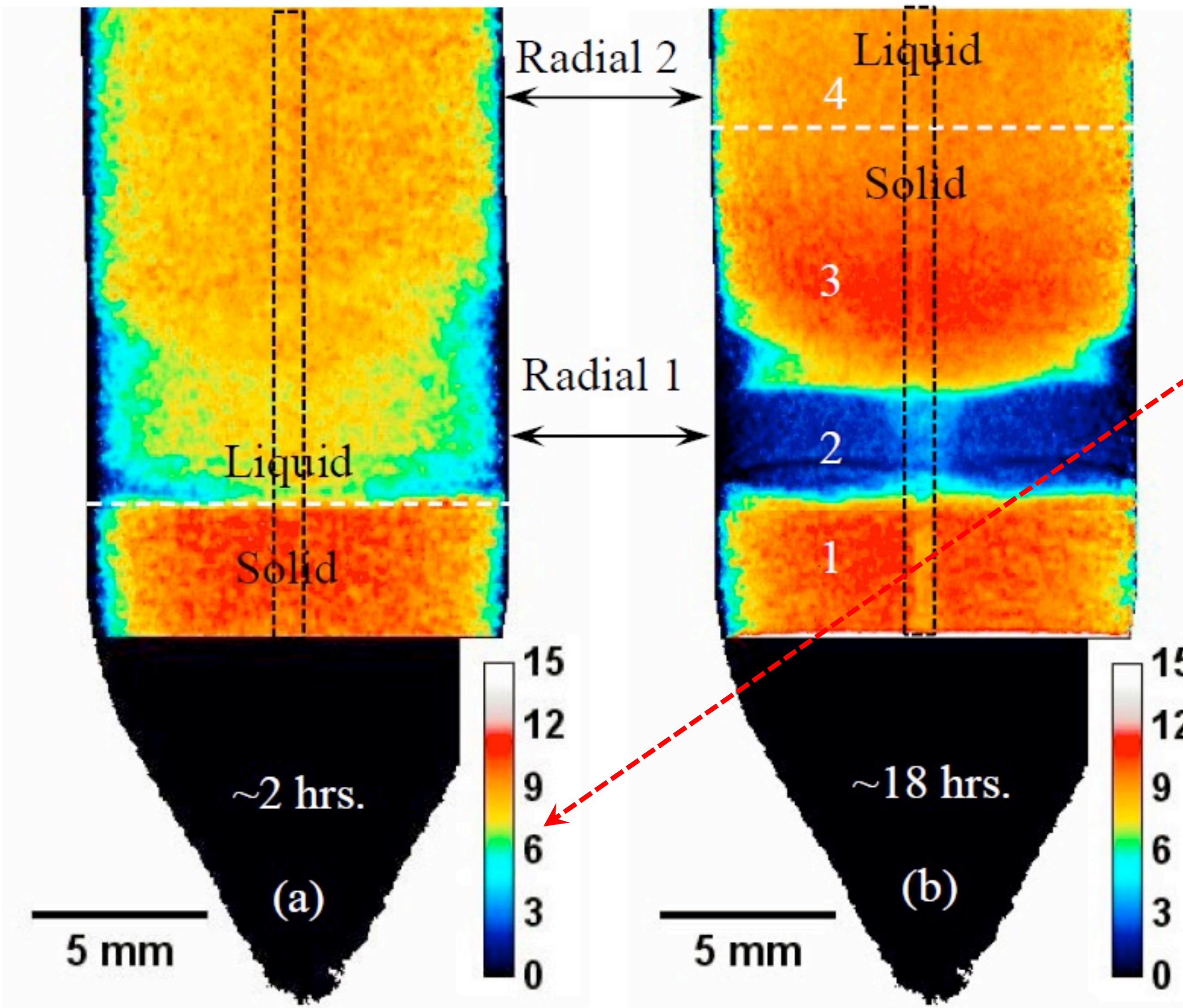

Color represents atom % concentration of Li within the ampule

Courtesy of Anton Tremsin (UC Berkeley)

Doping concentration at liquid/solid interface

In-situ Eu distribution quantification of BaBrCl:Eu

Courtesy of Anton Tremsin (UC Berkeley)

Scientific Reports 7 (2017) 46275

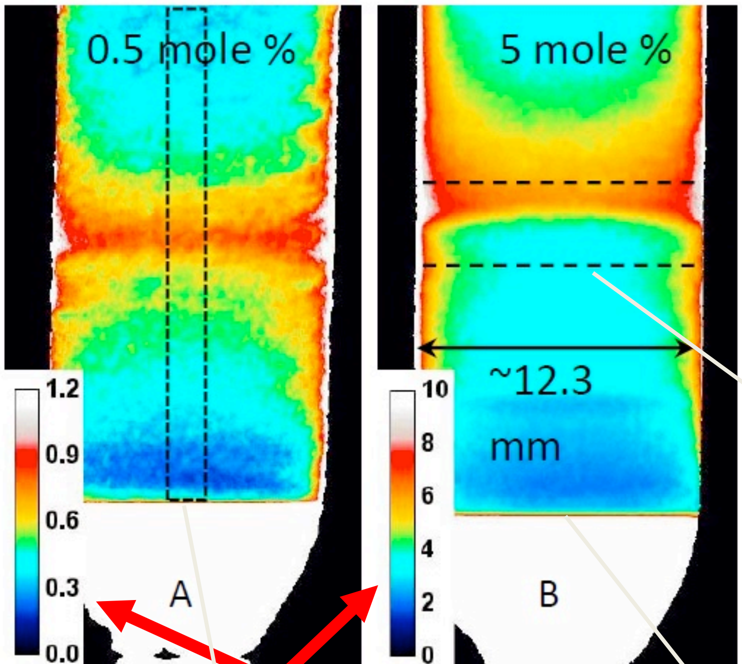

Eu concentration (mole %)

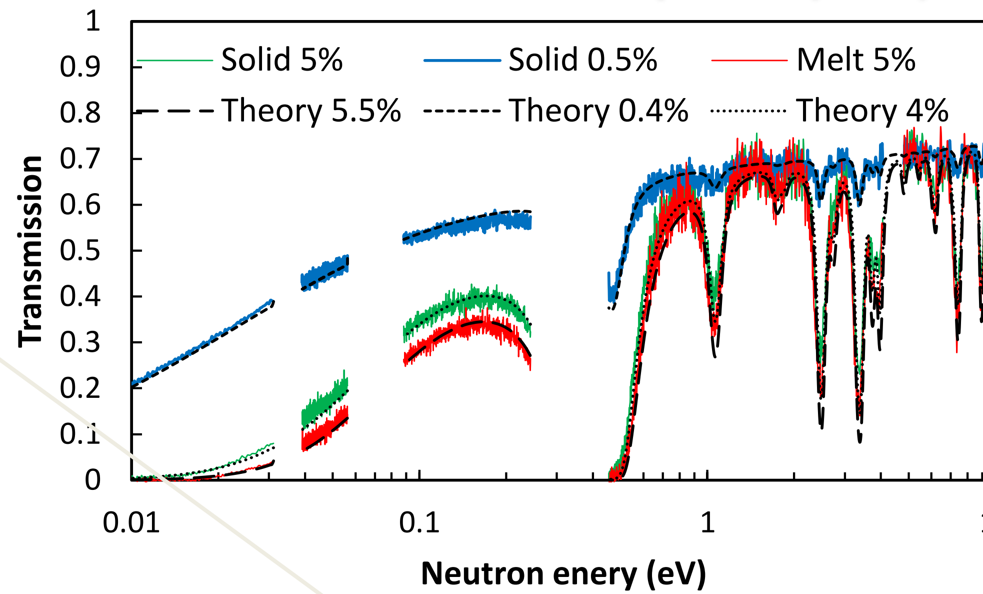

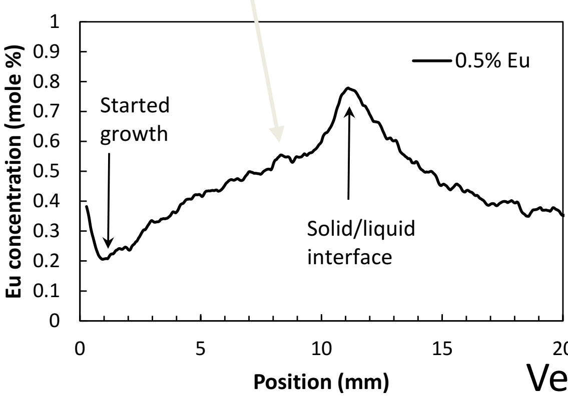

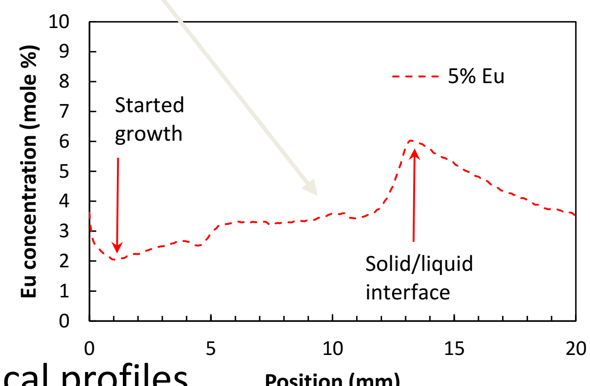

Vertical profiles

Radial profiles

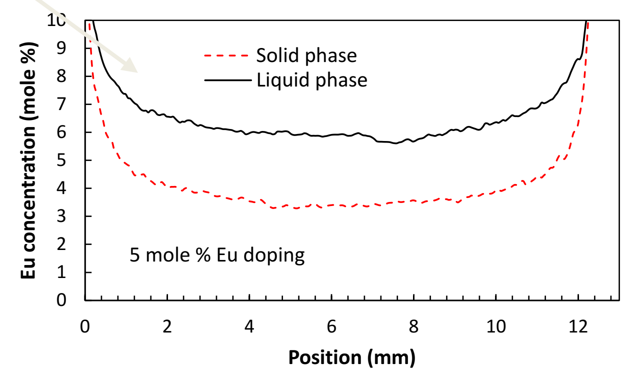

Grating based phase imaging

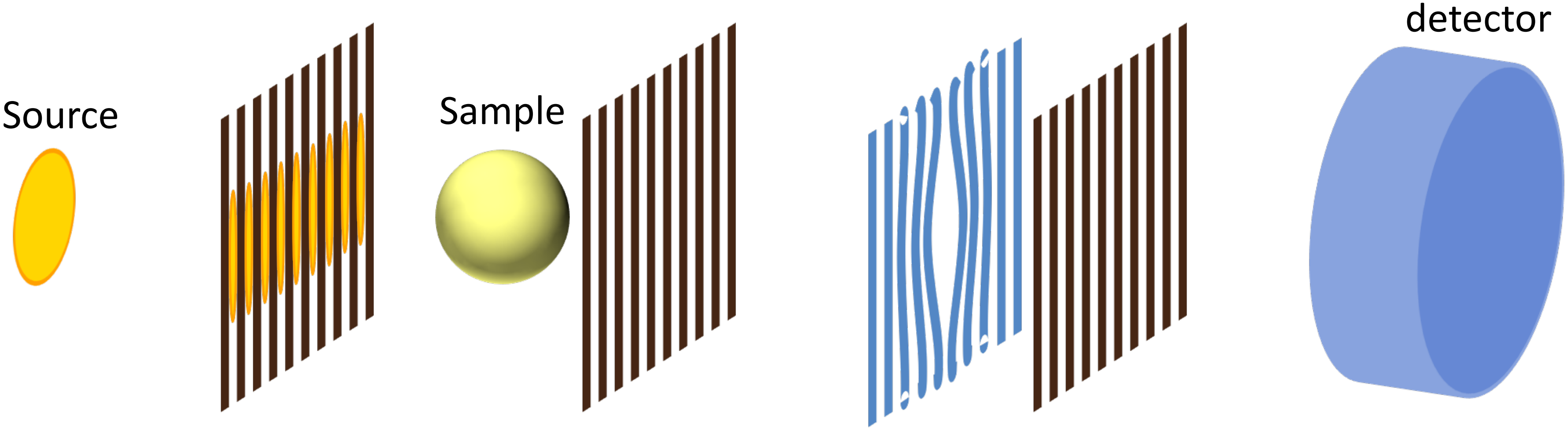

Talbot-Lau干渉イメージングの実験例（X-ray TLI 、試料：サクランボ)

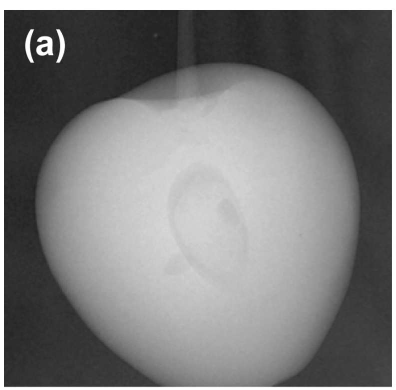

Absorption image
(absorption cross section)

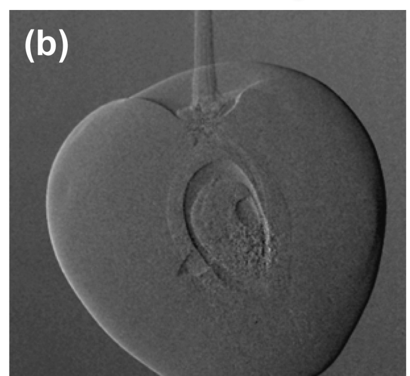

Differential phase image
(coherent scattering length)

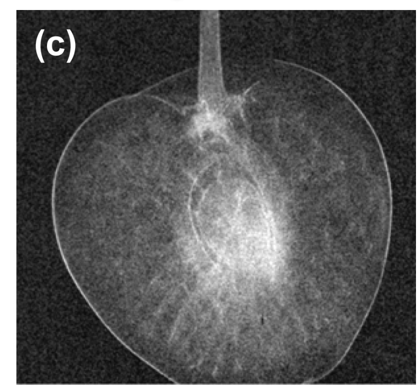

Visibility image
(small angle scattering)

Phase Imaging with neutrons

A neutron can sense optical potentials caused by nuclei and magnetic fields

	Nuclear	Magnetic
Optical potential U	$\frac{2\pi\hbar^2}{m} b_c \delta(\vec{r})$	$-\vec{\mu} \cdot \vec{B}(\vec{r})$
Phase shift Φ	$-N b_c \lambda D$	$\pm \frac{\mu B m \lambda D}{2\pi\hbar^2}$

Depending on the neutron polarity

N: number density
m: neutron mass
λ: wavelength
b_c: coherent scattering length
B: magnetic field
D: thickness

Nuclear potential → coherent scattering length and wavelength

Larger than absorption cross section

Magnetic potential → magnetic field strength and wavelength

Phase shift due to magnetic field

- ✓ Increase of sensitivity of neutron imaging
- ✓ Visualization of magnetic field distribution

Dark field signal relates to small angle scattering by micro structure.

→ Magnetic scattering is also analyzed.

Magnetic field sensitive phase imaging

Element	b_c [fm]	U_{nucl} [neV]	I_s [T]	U_{mag} [neV]
Si	4.15	116	0	0
Al	3.45	54	0	0
Fe	9.45	211	2.2	132
Ni	10.3	243	0.6	38
Magnetic field	0	0	1	60

Optical Potential *U* by magnetic field

$$-\vec{\mu} \cdot \vec{B}(\vec{r})$$

Optical potential *U* by *B* = 1 T
is same order with that by a nucleus.

Similar phase shift occurs by magnetic field. But it depends on the neutron polarity.

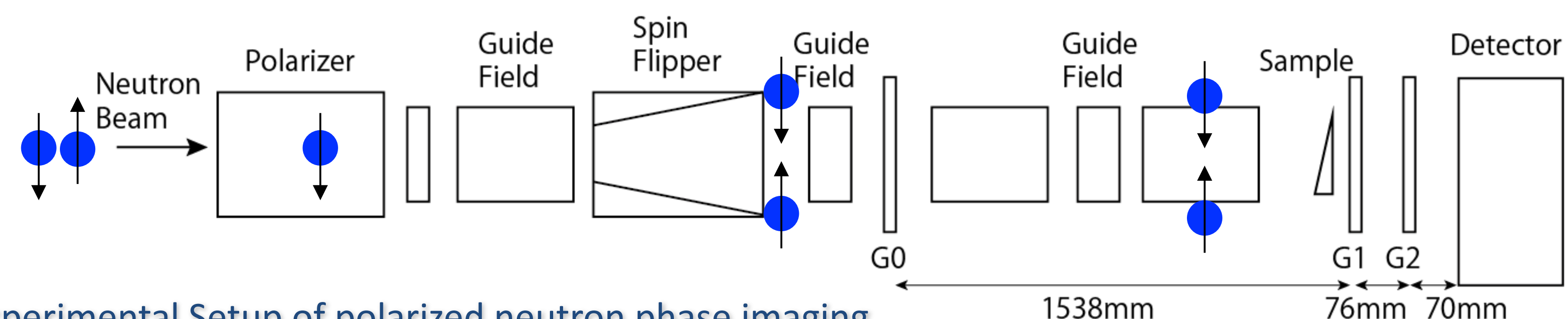

Experimental Setup of polarized neutron phase imaging

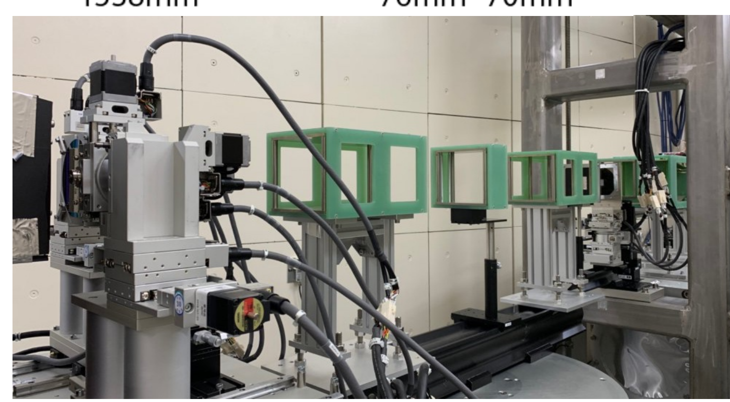

Flipping neutron spin polarity

Positive Spin : $U_{nucl} + U_{mag}$
Negative Spin : U_{nucl} - U_{mag}

Differential phase imaging using polarized neutron

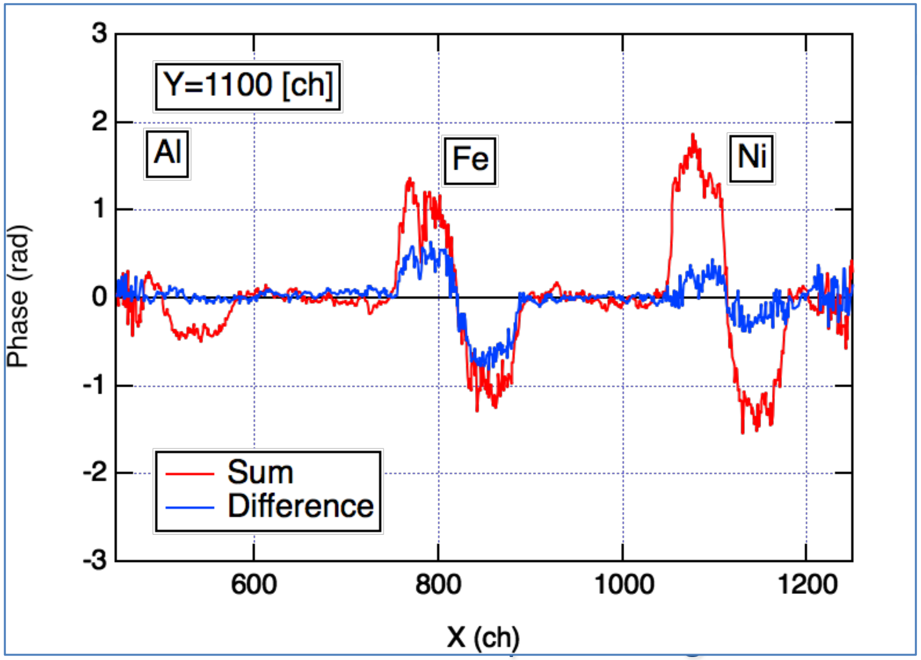

M **or** ***B*** **// ±*μ* // grating**

Positive Spin : $U_{nucl} + U_{mag}$
Negative Spin : $U_{nucl} - U_{mag}$

Difference : U_{mag} → Magnetic info.
Sum : U_{nucl} → Nuclear info.

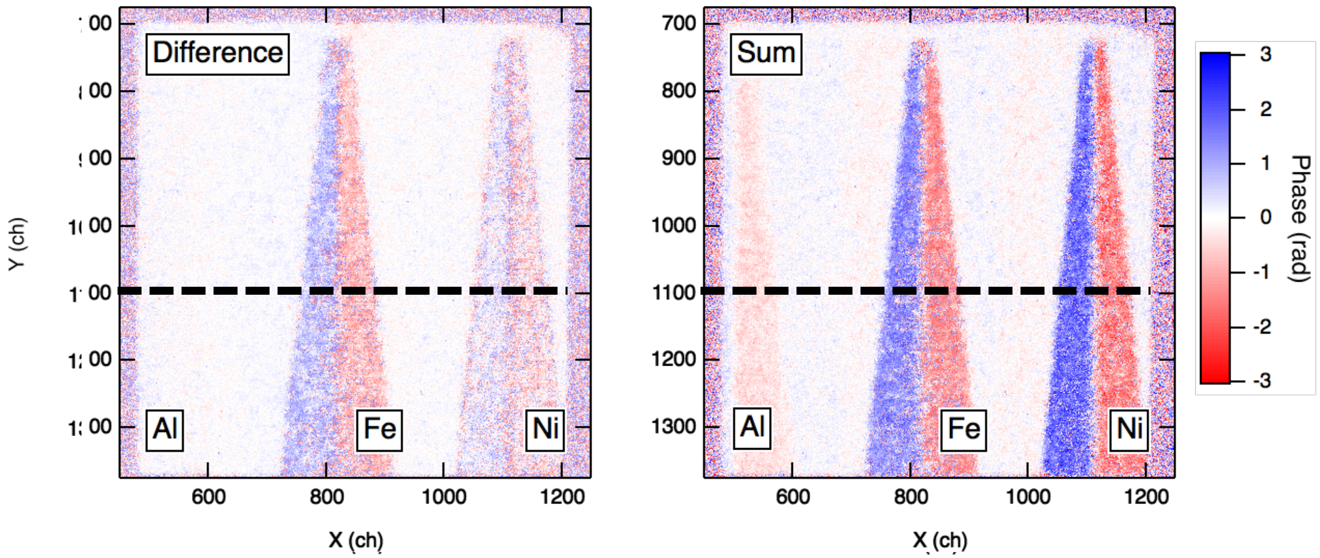

Visibility contrast by magnetic scattering

Magnetic scattering is maximum in case of $\boldsymbol{M} \perp \boldsymbol{q}$.

$\boldsymbol{M}$//grating ⟶ Sum of nuclear scattering and magnetic scattering

$\boldsymbol{M} \perp$ grating ⟶ No magnetic scattering contribution

Sample rotation by 90° = distinguish nuclear scattering and magnetic scattering.

Laser heated NdFeB magnet

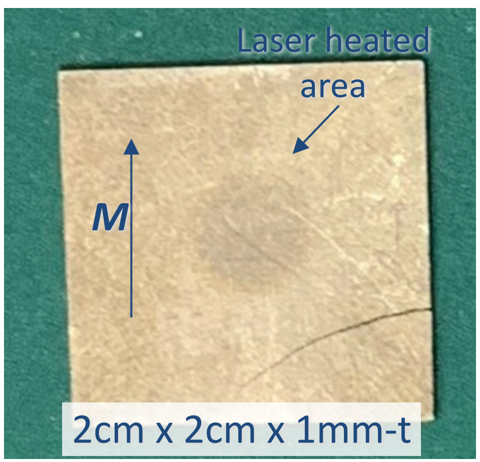

Central part was demagnetized by laser heating.

Visibility image ($\bar{\lambda}$ = 3.2 Å, $\Delta\lambda/\bar{\lambda}$ = 0.25)

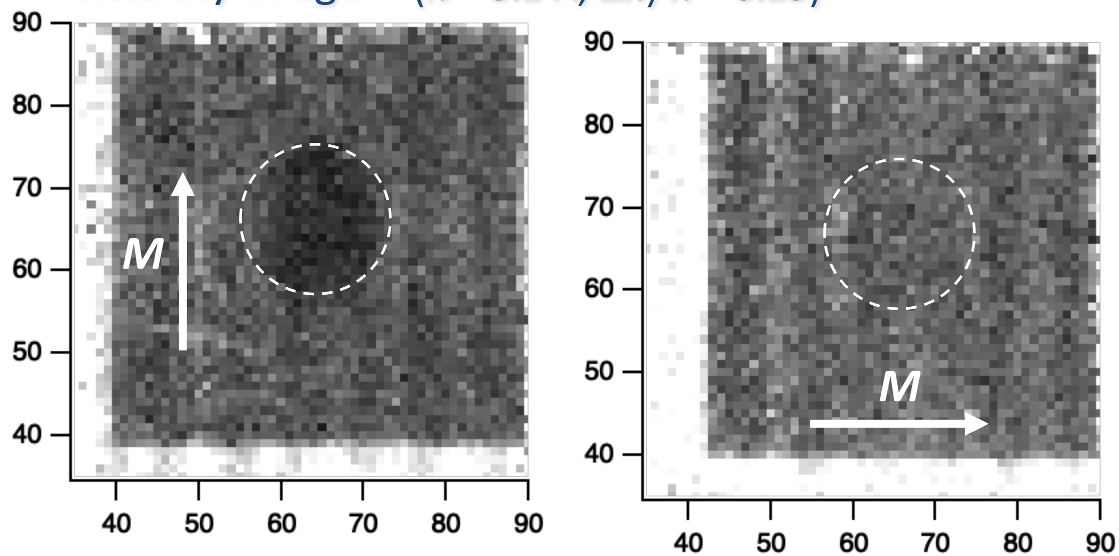

M//grating

M⊥grating

Visibility contrast by magnetic scattering

M//grating

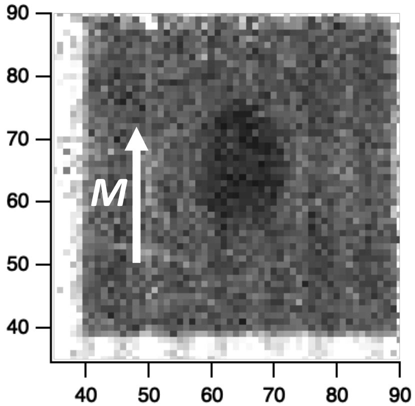

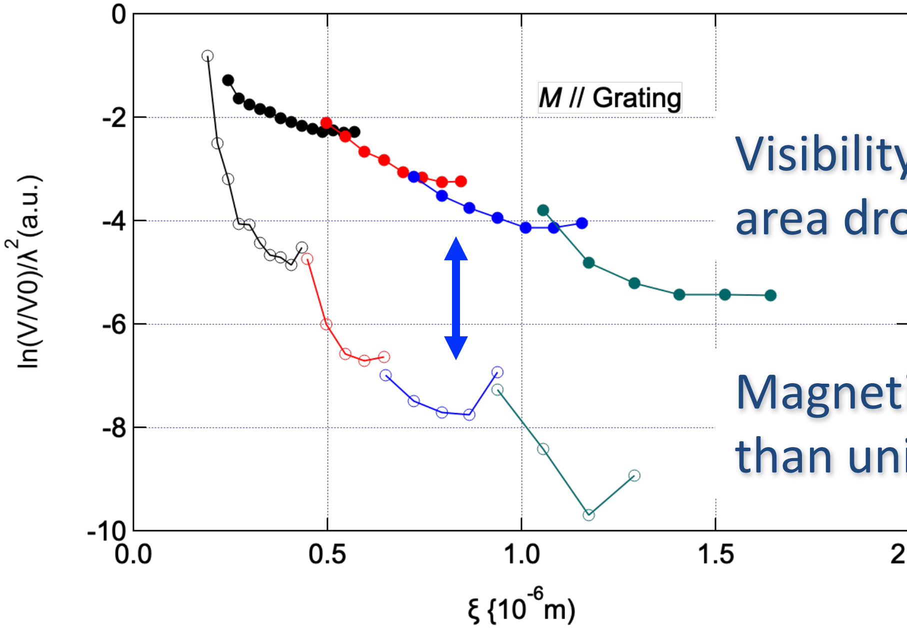

Visibility of laser irradiated area drops quickly.

Magnetic domain size is smaller than unirradiated area.

M⊥grating

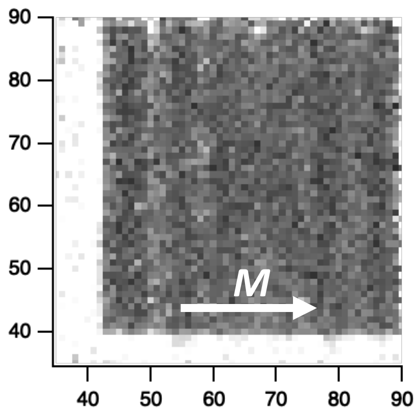

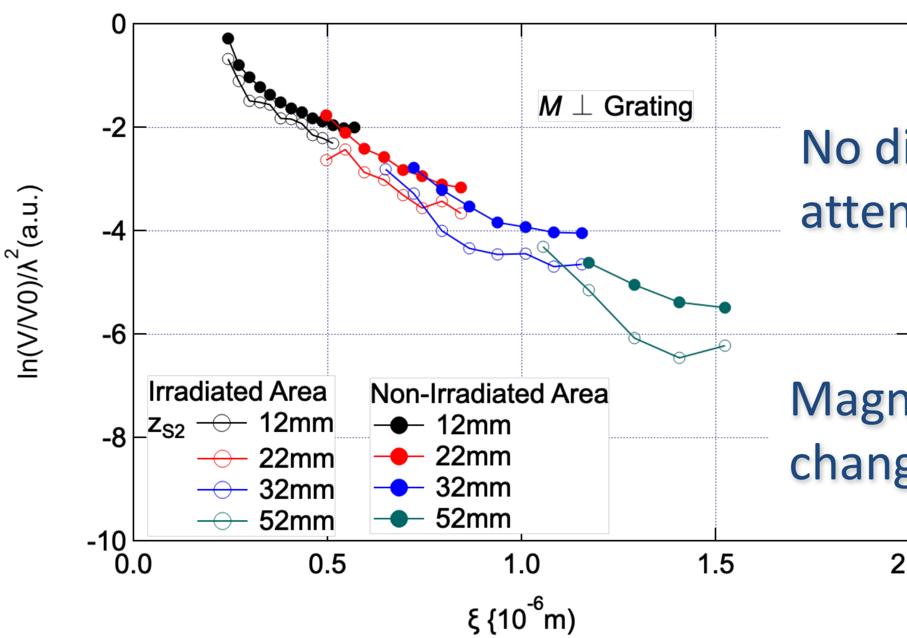

No difference in visibility attenuation.

Magnetization axis doesn't change by laser irradiation.

まとめ

- J-PARC/MLFのパルス中性子イメージング装置「螺鈿」は2015年より共用運転中
- エネルギー分析型中性子イメージング実験の本格的な実用化・応用研究を推進

- ブラッグエッジを利用した歪みトモグラフィや結晶成長過程の観察などの新しい技術開発・応用を長期課題で実施中。
- 位相イメージングの開発（ERATOプログラム）において、TOFとVisibility contrastを利用した磁性材料への応用を実施。

- 利用相談・研究協力は随時受け付けています

  実験に関する質問・技術開発や実験環境への要望

  →　遠慮なくお問い合わせ下さい

takenao.shinohara@j-parc.jp